Science of the Total Environment 874 (2023) 162366

Contents lists available at ScienceDirect

Science of the Total Environment

journal homepage: www.elsevier.com/locate/scitotenv

Developing a novel framework to re-examine half a century of compound drought and heatwave events in mainland China

Lin Zhao [a], Xinxin Li [a,*], Zhijiang Zhang [b], Moxi Yuan [c], Shao Sun [d], Sai Qu [a], Mengjie Hou [a], Dan Lu [a], Yajuan Zhou [a], Aiwen Lin [a]

[a] School of Resource and Environmental Sciences, Wuhan University, Wuhan 430079, China
[b] School of Geography Science and Geomatics Engineering, Suzhou University of Science and Technology, Suzhou 215009, China
[c] School of Public Administration and Human Geography, Hunan University of Technology and Business, Changsha 410205, China
[d] State Key Laboratory of Severe Weather (LASW), Chinese Academy of Meteorological Sciences, Beijing 100081, China

HIGHLIGHTS

- A novel framework for evaluating compound drought and heatwave events (CDHEs) is proposed.
- Assessing CDHEs on a daily scale facilitates the development of targeted risk management policies.
- Ignoring the precipitation attenuation effect and event merging significantly alters the spatial distribution and magnitude of the CDHEs.

GRAPHICAL ABSTRACT

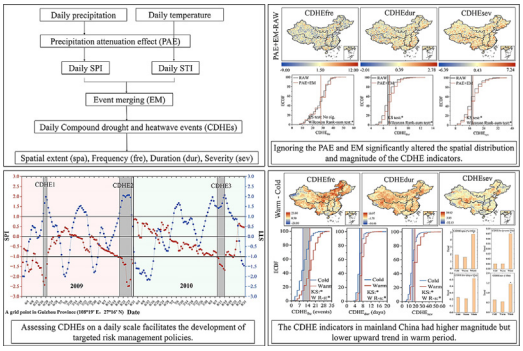

ARTICLE INFO

Editor: Ouyang Wei

Keywords:
CDHEs
Precipitation attenuation effect
Event merging
Daily scale assessment

ABSTRACT

Compound drought and heatwave events (CDHEs) are more devastating than single drought or heatwave events and have gained widespread attention. However, previous studies have not investigated the impacts of the precipitation attenuation effect (PAE) (i.e., the effect of previous precipitation on the dryness and wetness of the current system is attenuated) and event merging (EM) (i.e., merging two CDHEs with short intervals into a single event). Moreover, few studies have assessed short-term CDHEs within monthly scales and their variation characteristics under different background temperatures. Here we propose a novel framework for assessing CDHEs on a daily scale and considering the PAE and EM. We applied this framework to mainland China and investigated the spatiotemporal variation of the CDHE indicators (spatial extent ($CDHE_{spa}$), frequency ($CDHE_{fre}$), duration ($CHHE_{dur}$), and severity ($CDHE_{sev}$)) from 1968 to 2019. The results suggested that ignoring the PAE and EM led to significant changes in the spatial distribution and magnitude of the CDHE indicators. Daily-scale assessments allowed for monitoring the detailed evolution of CDHEs and facilitated the timely development of mitigation measures. Mainland China experienced frequent CDHEs from 1968 to 2019 (except for the southwestern part of Northwest China (NWC) and the western part of Southwest China (SWC)), whereas, hotspot areas of $CDHE_{dur}$ and $CDHE_{sev}$ had a patchy distribution in different geographical subregions. The CDHE indicators were higher in the warmer 1994–2019 period than in the colder 1968–1993 period, but the rate of increase of the indicators was lower or there was a downward trend. Overall, CDHEs in mainland China have been in a state of remarkable continuous strengthening over the past half a century. This study provides a new quantitative analysis approach for CDHEs.

* Corresponding author.
E-mail address: lixinxin_better@whu.edu.cn (X. Li).

http://dx.doi.org/10.1016/j.scitotenv.2023.162366
Received 8 December 2022; Received in revised form 15 February 2023; Accepted 17 February 2023
Available online 26 February 2023
0048-9697/© 2023 Elsevier B.V. All rights reserved.

1. Introduction

The impact of compound drought and heatwave events (CDHEs) on social-ecological systems exceeds that of individual drought or heatwave events and the sum of their impacts, even if the individual events are not extreme (Bevacqua et al., 2022; Leonard et al., 2014). Therefore, CDHEs have gained much attention for possessing this disproportionate destructiveness (Ridder et al., 2020; Zscheischler et al., 2018). Many regions worldwide have experienced severe CDHEs in recent years, such as the United States (Alizadeh et al., 2020; Hao et al., 2020b; Mazdiyasni and AghaKouchak, 2015), Europe (Manning et al., 2019; Sutanto et al., 2020), China (Liu and Zhou, 2021; Wu et al., 2020, Wu et al., 2019), Australia (Mu et al., 2021), India (Guntu and Agarwal, 2021; Sharma and Mujumdar, 2017), South Africa (Hao et al., 2020a; Hao et al., 2019), and southeastern Brazil (Geirinhas et al., 2021). These events have resulted in reduced crop yields (Feng et al., 2021; Hamed et al., 2021; Li et al., 2022; Ribeiro et al., 2020), forest and grassland wildfires (Guion et al., 2022; Witte et al., 2011), reduced carbon sequestration capacity of ecosystems (Li et al., 2021c), destruction of public infrastructure (AghaKouchak et al., 2020; Turner et al., 2019; Zscheischler et al., 2020), and human and animal mortality (Grumm, 2011; Shaposhnikov et al., 2014), posing significant risks to the ecological environment and human socio-economic development. More importantly, persistent global warming is changing the climate system and accelerating the variability of climate variables, such as temperature and precipitation. The frequency and severity of CDHEs are showing an increasing trend (Ridder et al., 2022; Zhou et al., 2019). Therefore, there is an urgent need to conduct an in-depth study of the occurrence and evolution of CDHEs to mitigate their adverse consequences.

Previous studies have revealed many insights into the evolution and impact of CDHEs, but most used a monthly scale or longer time scales to identify drought, representing the average dry and wet state of a region in a certain period. Thus, they could not identify short-term drought events (Feng et al., 2021, Feng et al., 2020; Otkin et al., 2018). Long-term drought and heat conditions (e.g., months or years) are useful for agricultural and socioeconomic planning. Decision makers in agriculture and other water-related sectors also want to know the current drought and heat conditions in an area. In contrast, CDHEs characterize the hydrometeorological state of the land-atmosphere system and are more suitable for describing events in more detail (Lu, 2009). More importantly, persistent global warming has resulted in CDHEs that occur suddenly and persist for days or weeks. Despite their short duration, they can devastate crops if they occur during periods when the crop has high water and heat requirements (Li et al., 2020a; Pendergrass et al., 2020; Yuan et al., 2019). Thus, daily scale assessment of CDHEs will help us understand the detailed evolution of these complex events to formulate timely mitigation strategies.

Previous studies have commonly used drought indices, such as the standardized precipitation index (SPI), standardized precipitation evapotranspiration index (SPEI), and Palmer Drought Severity Index (PDSI), to characterize drought information. However, they gave equal weight to the influence of previous precipitation on the current dry and wet state, ignoring the impacts of the precipitation attenuation effect (PAE) (i.e., the effect of previous precipitation on the dryness and wetness of the current system is attenuated) (Chen et al., 2019b; Wu et al., 2020). Specifically, the degree of dryness or wetness of a system on a given day depends on the precipitation on that day and on previous days, whereas the contribution of precipitation on earlier days is attenuated due to the water balance requirement, i.e., runoff, evapotranspiration, and percolation (Lu, 2009). Thus, it is more reasonable to assign a gradually decreasing weight to the previous precipitation. Some studies have considered the PAE to investigate single drought events in the Pearl River Basin in southern China and the Mississippi River Basin in the United States, and obtained valuable research results (Li et al., 2020b; Lu, 2009). We are inspired by these studies and believe that the research gap can be filled if PAEs are considered in the assessment of CDHEs.

Moreover, studies have suggested that CDHEs separated by short intervals are independent (Li et al., 2021a,b; Wu et al., 2019). However, CDHEs can have cumulative effects on vulnerable systems. For example, Curriero et al. (2002) demonstrated the possible epidemiological significance of a mitigation period of less than four days between heatwave events. Other studies have investigated the cumulative impact of precipitation deficits or high-temperature stress on ecosystems (Wen et al., 2019; Wu et al., 2015). However, no study has investigated the effect of event merging (EM) caused by the cumulative impact of CDHEs. Finally, many studies have divided long-term time-series data into two or more periods of equal length, ignoring the influence of the background temperature on the evolution of CDHEs (Wang et al., 2021; Zhou and Liu, 2018).

This study proposes a novel framework for assessing CDHEs using a daily scale and considering the influence of the PAE and EM. This framework is applied to mainland China, a region with complex and diverse climate types, whose ecosystem and social development are vulnerable to climate extremes. We aim to answer the following questions: (1) What is the impact of the PAE and EM on the evaluation of CDHEs? (2) What are the advantages of monitoring CDHEs on a daily scale? (3) What are the differences in the spatiotemporal variation of CDHEs in different geographical subregions of mainland China? (4) How has climate warming affected CDHEs in mainland China? We hope that the results of this study can provide new insights into risk management of CDHEs in China. More importantly, we hope that the proposed CDHE assessment framework can provide a new perspective for the quantitative analysis of CDHEs.

2. Data and methods

2.1. Data

We used a gridded daily precipitation and mean temperature dataset (spatial resolution 0.5° × 0.5°) for mainland China from 1968 to 2019 produced by the National Meteorological Information Center (NMIC) of the China Meteorological Administration (CMA) (http://data.cma.cn/). The NMIC verifies the data quality and uniformity of 2472 station observations and GTOPO30 DEM data using the cumulative bias test and the standard normal homogeneity test. Spatial interpolation using the thin plate spline method is then used to derive the dataset (Fig. 1). This dataset has been used in several studies to evaluate drought and heatwave events (Li et al., 2021b; Lu et al., 2014).

2.2. Identification of drought events considering the PAE

This study quantifies drought on a daily scale and considers the PAE on the current system's dryness and wetness. To avoid an overlap with the temperature trends, we chose the SPI calculated using only precipitation to characterize drought (Shi et al., 2021). The World Meteorological Organization (WMO) recommends using the SPI to characterize meteorological drought. It is defined as the number of standard deviations the observed precipitation anomalies deviate from the long-term mean. It is suitable for quantifying drought under different climate regimes (Dai, 2012; Hayes et al., 2011; Robock et al., 2000). Following Li et al. (2020b), we chose a precipitation attenuation coefficient of 0.98. This study uses the gamma distribution to fit the precipitation time series (Stagge et al., 2015). The SPI is then obtained based on a Gaussian (normal) distribution transformation (Hao et al., 2021). In this study, the time scale of the SPI is 30 days because a short time scale is preferred to reflect the dryness/wetness of shallow soils (Wang et al., 2021). An SPI of ≤-1 for at least three consecutive days indicates a moderate-intensity drought event (Mukherjee and Mishra, 2021; Svoboda et al., 2002). The SPI calculation procedure that considers the PAE is described in the supplementary materials.

2.3. Identification of heatwave events

This study uses the standardized temperature index (STI) to identify heatwave events. A moving average window (7 d) is used to obtain the daily average temperature in the time series during the study period. A normal distribution function is then used to fit the temperature time series

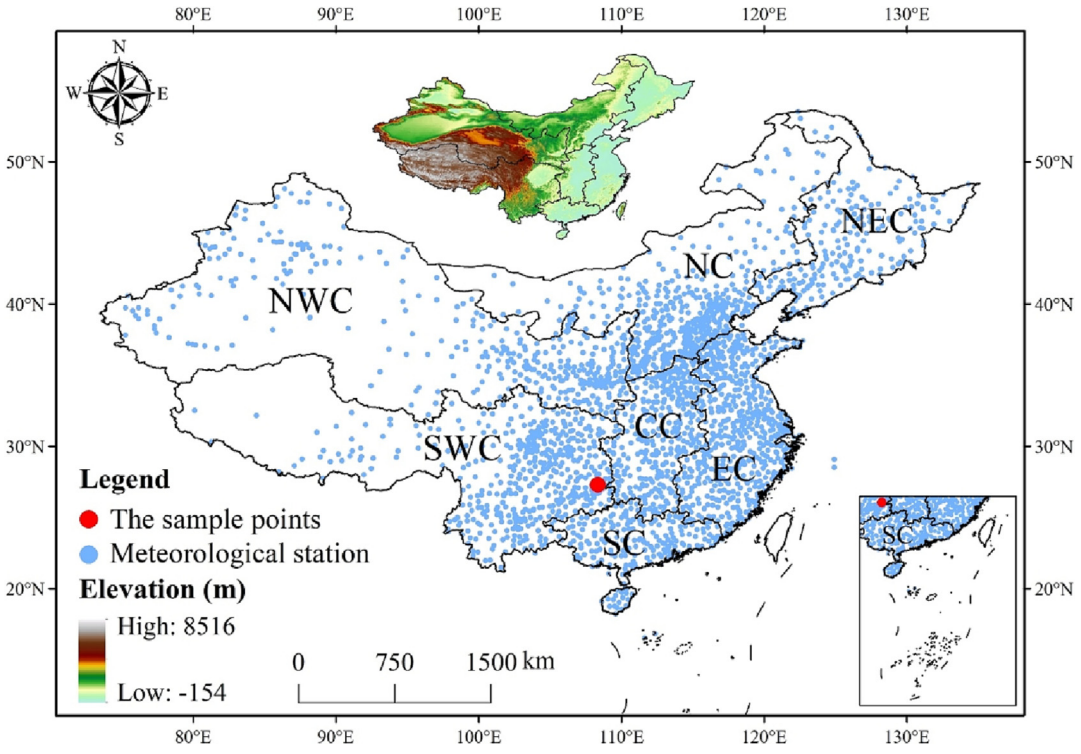

Fig. 1. Spatial distribution of meteorological stations in seven subregions in mainland China. According to the regional climate background and the current socio-economic development, mainland China is divided into seven subregions: Northwest China (NWC), Southwest China (SWC), North China (NC), Central China (CC), South China (SC), Northeast China (NEC), and East China (EC). The solid blue circles indicate meteorological stations. The small map at the top shows the elevation of the study area.

since related studies have shown that temperature anomalies are typically normally distributed (Hansen et al., 2012; Zscheischler et al., 2014). Finally, the cumulative distribution function $G(t)$ of the temperature time series is converted to the STI based on the standard normal distribution (Eqs. (1)–(2)) (Li et al., 2021b). We used the 7-d STI to identify short-term heatwave events, i.e., an STI ≥ 1 for at least three consecutive days indicates a heatwave event.

$$G(t) = \frac{1}{\sigma\sqrt{2\pi}} \int_{-\infty}^{T} exp\left(-\frac{(t-\mu)^2}{2\sigma^2} \right) dt \quad (1)$$

$$STI = \varphi^{-1}(q) \quad (2)$$

where t is the daily average temperature time series; μ and σ are the mean and standard deviation of the series, respectively; q is the cumulative probability; φ is the standard normal distribution.

2.4. Identification of CDHEs

A CDHE is defined as a drought event occurring simultaneously with a heatwave event, i.e., the SPI ≤ −1 and the STI ≥ 1 for at least three consecutive days. This approach is simple and effective for defining CDHEs and has been widely used (Feng et al., 2021; Li et al., 2021a,b). Following Mukherjee and Mishra (2021), we chose a merging thresholds of 4 days for compound events. i.e., two adjacent CDHEs are considered two independent events if they are at least four days apart; otherwise, they are merged into one event. We used the following four indicators to characterize CDHEs: (a) the spatial extent ($CDHE_{spa}$) is defined as the number of grids in which CDHEs occur in any given year as a percentage of the total number of grids. (b) The frequency ($CDHE_{fre}$) is defined as the total number of CDHEs occurring in any given year for a given grid. (c) The duration ($CDHE_{dur}$) is defined as the total number of days of observed CDHEs for a grid in any given year divided by the $CDHE_{fre}$. (d) The severity ($CDHE_{sev}$) is obtained by calculating the product of the SPI and STI for each day and each grid during each CDHE in any given year. The products are summed, and the absolute value is divided by the $CDHE_{fre}$ to obtain the $CDHE_{sev}$ (Hao et al., 2022; Mukherjee and Mishra, 2021). This study focused only on CDHEs in the summer (June–August) from 1968 to 2019, because CDHEs substantially affect water availability and energy expenditure in summer (Hao et al., 2020a). The process of identifying CDHEs is shown in Fig. 2.

2.5. Division into cold and warm periods

We identified warmer periods based on the annual average summer temperature anomalies in mainland China from 1968 to 2019 (Fig. 3). The anomalies were evaluated for each grid relative to the long-term average from 1968 to 2019, and spatial averaging was performed for mainland China. Fig. 3 shows that 1994–2019 was much warmer than 1968–1993, as evidenced by the persistent negative temperature anomalies in 1968–1993 (except for 1988 and 1991) and the persistent positive temperature anomalies observed since 1994 (except for 1995, 1996, and 2003). In general, this phenomenon may be the result of a combination of natural climate forcing (e.g., changing atmospheric circulation patterns) and anthropogenic climate forcing (e.g., enhanced human activities) (Hao et al., 2022).

2.6. Statistical analysis

In this study, the Trend free Pre-Whitening method (TFPW) was used to remove the time series correlation of the $CDHE_{spa}$, $CDHE_{fre}$, $CDHE_{dur}$ and $CDHE_{sev}$ (Yue and Wang, 2002). Interannual trends of the CDHE indicators were estimated by using Sen's slope estimator (Sen, 1968), and the significance was evaluated using the Mann-Kendall (MK) trend test (Kendall, 1975; Mann, 1945) under the null hypothesis of no trend. The two-sample Kolmogorov-Smirnov (KS) test and the Wilcoxon Rank-sum test were used to assess differences in the distribution and median, respectively, of the CDHE indicators for 1968–1993 and 1994–2019 for different

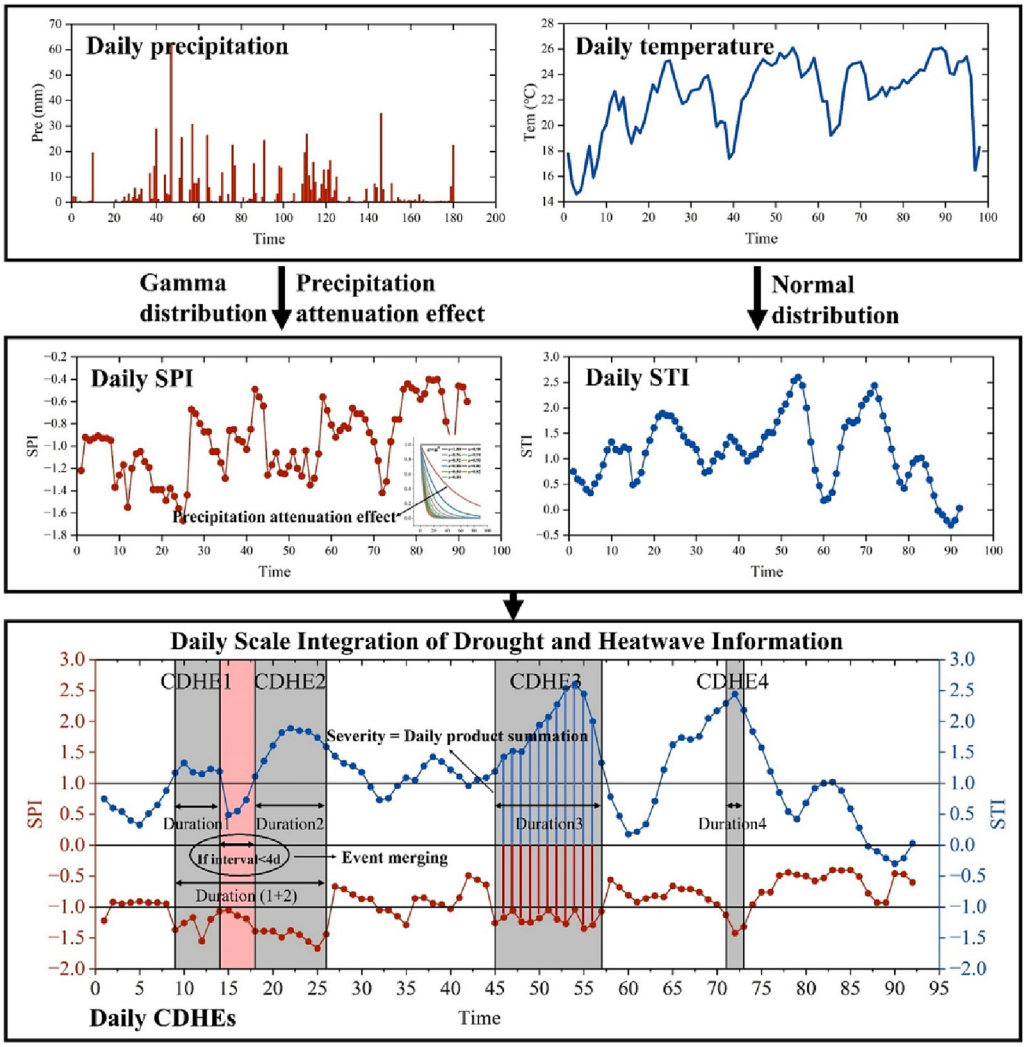

Fig. 2. Flow chart of daily scale CDHEs assessment considering PAE and EM. PAE and EM represent the precipitation attenuation effect and event merging, respectively.

geographical subregions in mainland China (Alizadeh et al., 2020; Mukherjee and Mishra, 2021). The test indicates whether the data from the two periods have the same distribution at a 0.05 significance level. Pearson correlation analysis was conducted to evaluate the effect of the merging threshold and precipitation attenuation coefficient on CDHEs (Lee Rodgers and Nicewander, 1988).

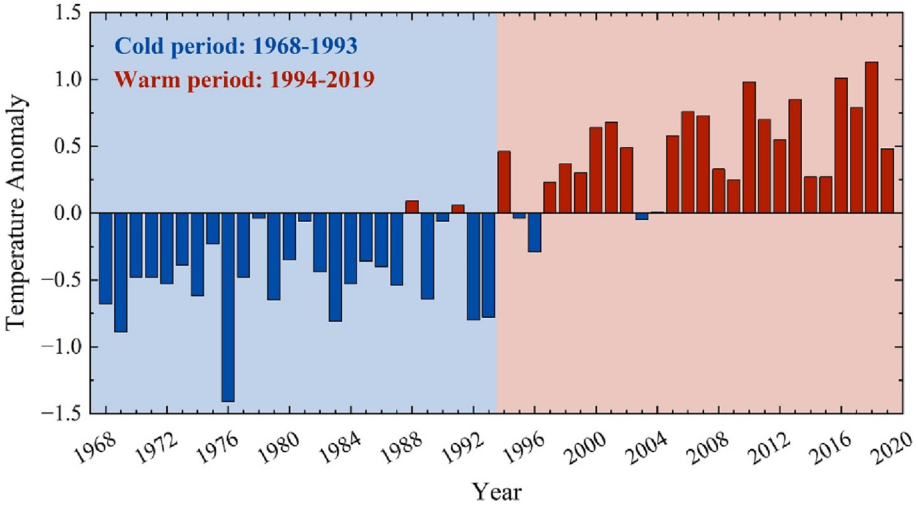

Fig. 3. Anomalies in the mean summer temperature from 1968 to 2019 relative to the long-term average (1968–2019).

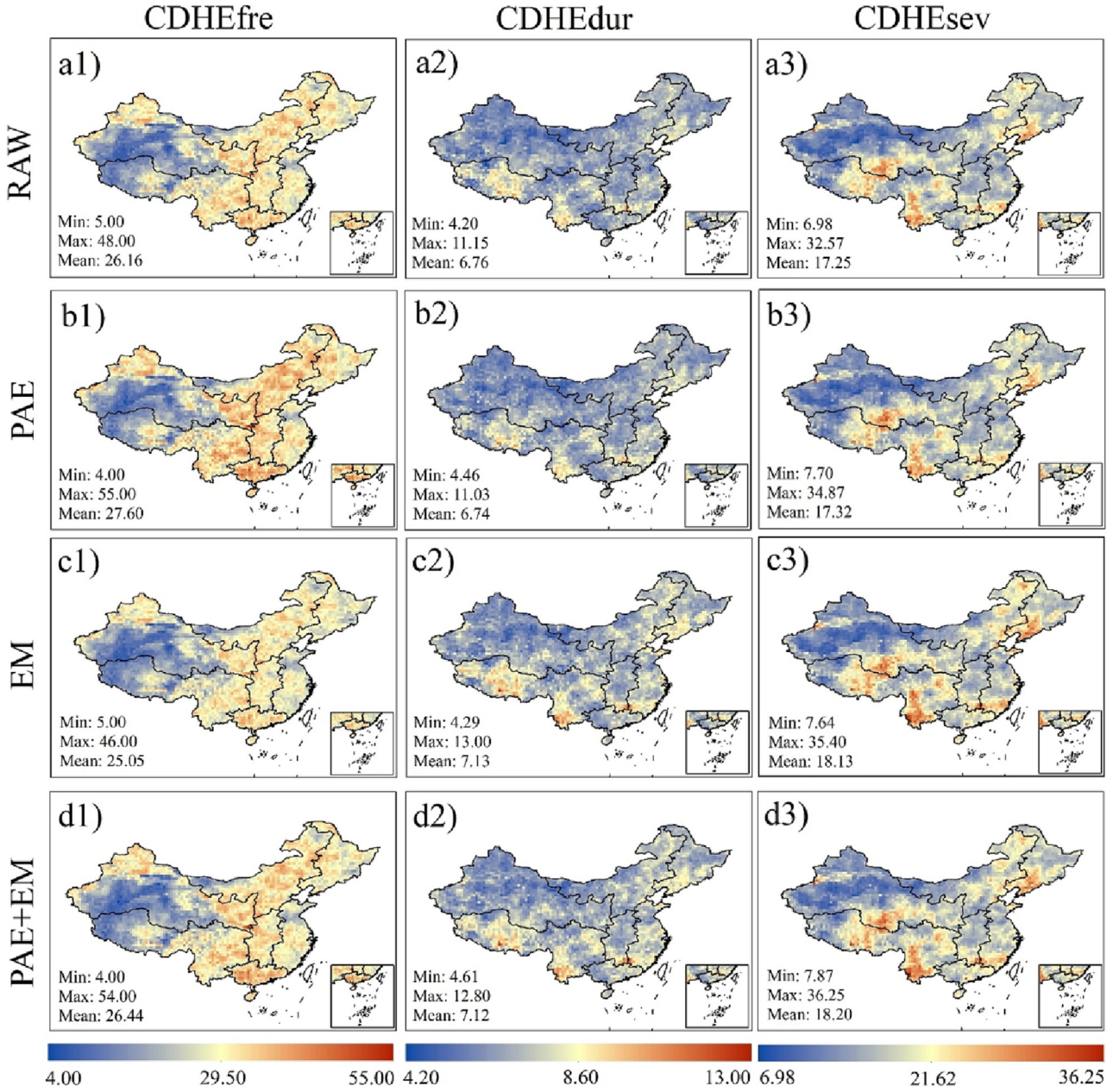

Fig. 4. Spatial distribution of CDHEs in mainland China from 1968 to 2019. a1)-a3) the PAE and EM are not considered. b1)-b3) only the PAE is considered. c1)-c3) only EM is considered. d1)-d3) PAE and EM are considered. PAE and EM represent the precipitation attenuation effect and event merging, respectively. The precipitation attenuation coefficient and the merging threshold are 0.98 and 4, respectively.

3. Results

3.1. Influence of the PAE and EM on CDHEs

Regardless of whether the PAE and/or EM were considered, the average CDHE indicators in mainland China during 1968–2019 had a similar spatial distribution with strong spatial heterogeneity, but the amplitude of the average CDHE indicators was different (Fig. 4). Except for the southwestern part of the NWC and the western part of the SWC, all other regions in mainland China had high values of $CDHE_{fre}$. The $CDHE_{dur}$ and $CDHE_{sev}$ were higher in the Ili River basin of NWC, the central junction of NWC and SWC, the southeast and northeast corners of SWC, the junction of CC, SC and EC, the northeast corner of EC, the southern part of NEC, and the northeastern part of NC (Fig. 4 (d1-d3)). The difference in the average CDHEs in different geographic subregions of mainland China can be partially attributed to the fact that the occurrence and evolution of drought and heatwaves are controlled by multiple surface fluxes (Mishra and Singh, 2010), whose spatial patterns are heterogeneous due to regional differences in precipitation and temperature anomalies and changes in other hydrologic variables (Konapala and Mishra, 2020; Kumar et al., 2016). In addition, these surface fluxes are influenced by background aridity, anthropogenic factors, and changes in large-scale climate patterns (Mukherjee et al., 2020; Sankarasubramanian et al., 2020).

Fig. 5 shows the difference in the spatial distribution of the CDHE indicators in mainland China from 1968 to 2019 between not considering the PAE and EM and considering one or both. The results showed that the average CDHE indicators increased or decreased in magnitude in most regions of mainland China after considering PAE and/or EM, but the percentage of regions that increased or decreased depended on the number of factors,

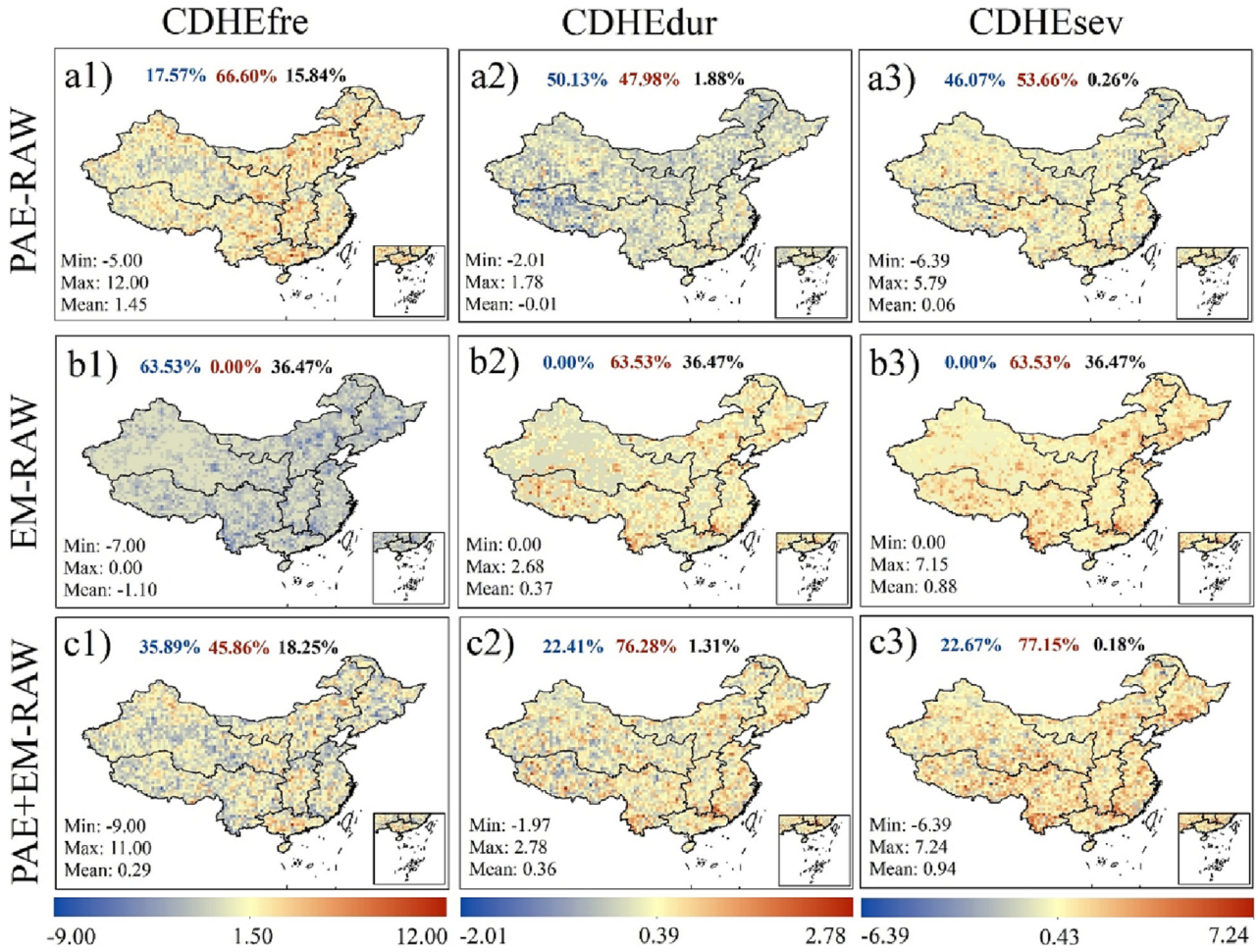

Fig. 5. Difference in the spatial distribution of CDHEs in mainland China from 1968 to 2019 between not considering the PAE and EM and considering one or both. PAE and EM represent the precipitation attenuation effect and event merging, respectively. The percentages of the blue, red, and black numbers above the subgraphs indicate a decrease, increase, and no change in the spatial extent, respectively.

the consideration of PAE and/or EM, and the type of CDHE indicators. Furthermore, when PAE and/or EM were considered, the variation in the magnitude of the CDHE indicators in mainland China was not spatially uniform and highly heterogeneous.

We investigated the difference and statistical significance of the median and spatial distribution of the CDHE indicators in mainland China without considering the PAE and EM, only considering the PAE, only considering EM, and considering the PAE and EM (Fig. 6). When only the PAE was considered, the curve of the empirical cumulative density function (ECDF) of the $CDHE_{fre}$ moved significantly in the positive direction, and the median value significantly increased from 28.00 to 29.00. In contrast, the ECDF curve and median value of the $CDHE_{dur}$ did not change significantly. The ECDF curve of the $CDHE_{sev}$ moved significantly in the negative direction, but the median value did not change significantly. When only the EM was considered, the ECDF curve of the $CDHE_{fre}$ shifted significantly in the negative direction, and the median value decreased significantly from 28.00 to 27.00. The ECDF curves of the $CDHE_{dur}$ and $CDHE_{sev}$ shifted significantly in the positive direction. The median $CDHE_{dur}$ increased significantly from 6.68 to 7.02, and that of $CDHE_{sev}$ increased significantly from 17.05 to 17.81. When the PAE and EM were considered, the median $CDHE_{fre}$ did not change significantly, but the ECDF curve was significantly different. The ECDF curves of the $CDHE_{dur}$ and $CDHE_{sev}$ shifted significantly. The median $CDHE_{dur}$ increased significantly from 6.68 to 7.00, and the median $CDHE_{sev}$ increased significantly from 17.05 to 17.91. The results indicate that ignoring the PAE and EM significantly changed the ECDF curve and magnitude of the CDHE indicators. Therefore, it is necessary to incorporate the PAE and EM into the CDHE assessment framework.

3.2. Daily scale CDHE monitoring

A once-in-a-century drought event occurred in five provinces in SWC from 2009 to 2010 (including Yunnan, Guizhou, Guangxi, Sichuan, and Chongqing) (Li et al., 2019). We selected a grid point in Guizhou Province (the red sample points in Fig. 1, 108°19′ E, 27°16′ N) and calculated the daily STI and SPI considering the PAE at this point from June to August in 2009 and 2010. Drought occurred at this location starting in June 2009. The drought intensified from June 1 to June 20, followed by a reduction in intensity until July 15 and an increase from July 16 to August 31 (Fig. 7 (a-b)). The daily scale drought evolution observed in this study is in good agreement with Lu et al. (2011), indicating that the proposed SPI drought index considering the PAE is robust for monitoring drought. We found that CDHEs with moderate intensity occurred three times in the summers of 2009 and 2010 at this grid point. CDHE1 occurred from June 18 to June 21, 2009, lasting for 4 days. CDHE2 occurred from August 20 to August 30, 2009 and lasted for 11 days. CDHE3 occurred from August 9 to August 15, 2010 and lasted for 7 days.

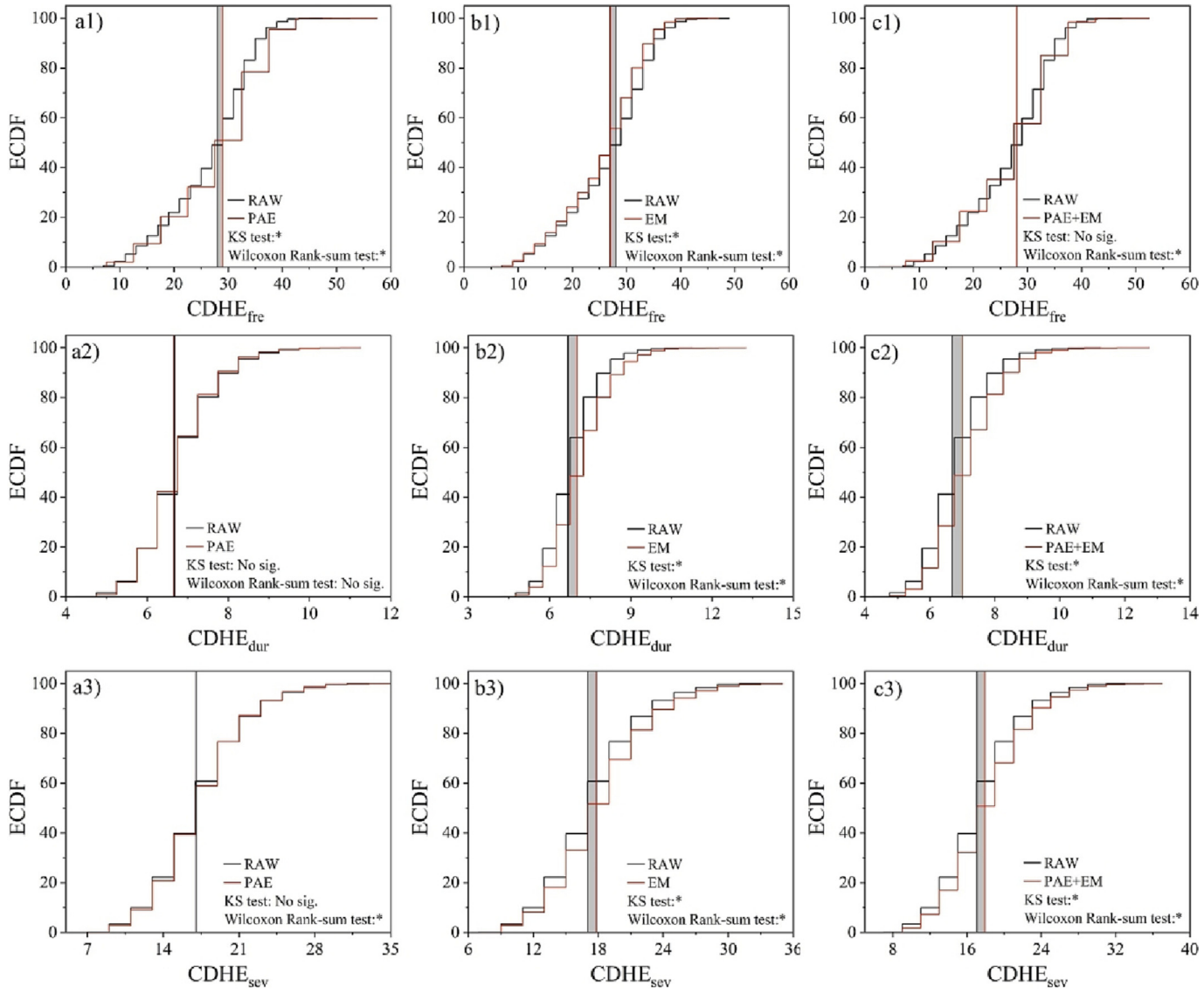

Fig. 6. Statistically significant changes in the empirical cumulative density function (ECDF) and median of the CDHE indicators in mainland China from 1968 to 2019 before and after considering the PAE and EM. "*" in the lower right corner of each subgraph indicates that the difference is significant at the $p = 0.05$ level. The black and red horizontal step lines indicate the ECDF before and after considering the parameters, respectively. The black and red vertical lines indicate the median before and after considering the parameters, respectively.

In addition, we calculated the SPI and STI at this location on a monthly scale from June to August in 2009 and 2010 (Fig. 7(c-d)). The trends of the SPI and STI at the monthly scale were consistent with those at the daily scale in the two consecutive summers. However, CDHE1 in June 2009 and CDHE3 in August 2010 were not detected on the monthly scale. Although August 2009 was identified as a hot and dry month on the monthly scale, the start and end dates of the specific CDHE2 could not be identified due to the coarse scale. The key advantage of daily over monthly CDHE monitoring is that CDHEs can be detected at a finer scale.

3.3. Spatiotemporal variation of CDHEs

The average CDHE$_{fre}$, CDHE$_{dur}$ and CDHE$_{sev}$ in mainland China were 10.44 events, 6.38 days and 15.38 in 1968–1993 and 16.00 events, 7.58 days and 19.91 in 1994–2019, respectively. The CDHE indicators in mainland China had higher values in 1994–2019 than in 1968–1993, and their spatial distribution was highly similar to that of 1968–1993 (Fig. 4 (d1-d3)). Quantitative analysis showed that 79.55 % of the regions experienced more frequent CDHEs (1–25 more events, with an average of 5.56 events), 74.53 % experienced more persistent CDHEs (1.00–10.97 more days, with an average of 1.19 days) and 76.44 % experienced more severe CDHEs (an increase of 1.00–39.82, with an average of 4.54) in 1994–2019 thin in 1968–1993. There were differences in the percentage of regions with increased magnitudes of CDHE indicators in the seven geographic subregions (62.09 %–97.15 % for CDHE$_{fre}$, 45.75 %–84.56 % for CDHE$_{dur}$, and 45.75 %–91.90 % for CDHE$_{sev}$).

We quantified the differences in the spatial distribution and median of the CDHE indicators in the warmer periods relative to colder periods using the KS test and Wilcoxon Rank-sum test, respectively, to assess whether climate warming had a significant effect on the spatiotemporal variation of the CDHE indicators. We calculated the average of the 26-year magnitude of the CDHE indicators in each of the two periods. We investigated the spatiotemporal variation of the CDHE indicators during the colder and warmer periods by comparing the ECDFs and medians of the average CDHE indicators (Fig. 9).

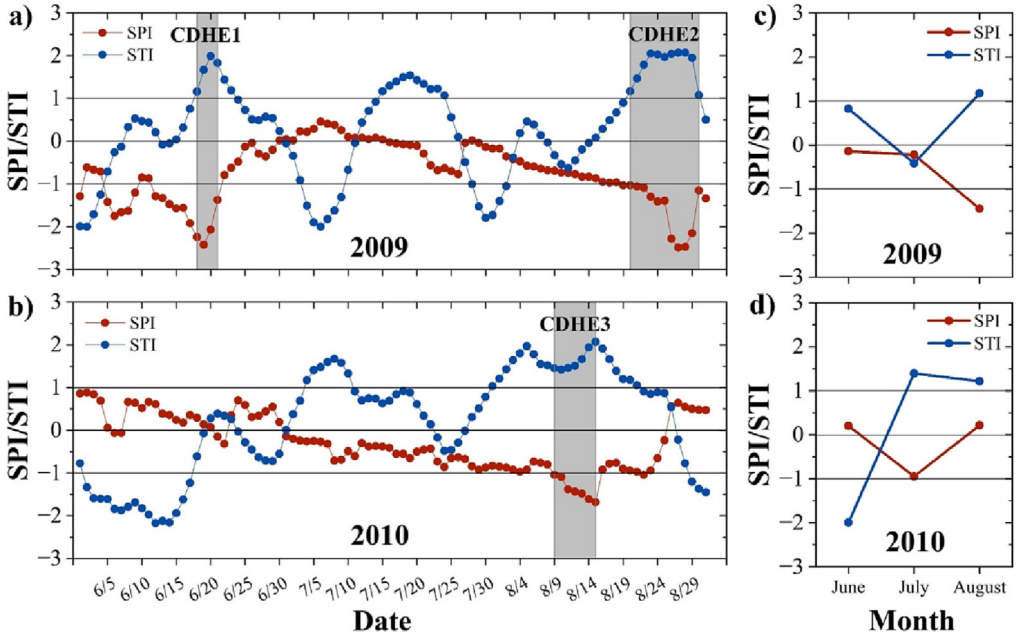

Fig. 7. Daily scale CDHE monitoring of a location in Guizhou Province, China (the red sample points in Fig. 1, 108°19′ E, 27°16′ N) during summers in 2009 and 2010.

The ECDF curve and median of the mean $CDHE_{fre}$, $CDHE_{dur}$, and $CDHE_{sev}$ in mainland China shifted significantly in the positive direction (95 % confidence level) during the more recent warmer period of 1994–2019. The median difference in the CDHE indicators was 6.00 events ($CDHE_{fre}$), 1.10 days ($CDHE_{dur}$), and 4.11 ($CDHE_{sev}$), respectively. In particular, a positive change in the median of $CDHE_{fre}$ occurred in the NC (11 events) and NEC (7 events), exceeding that of mainland China. In addition, SWC, NC, and EC exhibited longer $CDHE_{dur}$ in the warmer period than in the colder period, with a median difference of 1.47 days, 1.39 days, and 1.26 days between the two periods, respectively, exceeding that of mainland China. The $CDHE_{sev}$ in SWC and NC was higher than in mainland China in the warmer period than in the colder period, with a median difference of 4.88 and 6.20, respectively. We observed that the $CDHE_{fre}$ in SC had the smallest median difference (2.00 events) between the two periods among the seven geographic subregions, whereas the $CDHE_{dur}$ and $CDHE_{sev}$ showed no significant difference in the spatial distribution and median between the colder and warmer periods. Although the magnitude of the difference in the median CDHE indicators between the two periods was lower in NWC and CC than in mainland China, it was significant at the 95 % confidence level. Overall, mainland China was exposed to more frequent, persistent and severe CDHEs from 1994 to 2019, as indicated by the statistically significant increases and positive shifts in the median and ECDF curves of the CDHE indicators. However, these changes were not consistent in the seven geographic subregions, probably due to regional differences in the rate of change of climate variables, such as precipitation and temperature, although warming has continued to alter the recent climate system in mainland China (Konapala and Mishra, 2020; Kumar et al., 2016).

Overall, CDHEs in mainland China have consistently strengthened over the past half a century, as evidenced by the upward trend of the CDHE indicators in 1968–1993, 1994–2019, and 1968–2019. However, the magnitude of the upward trend of each indicator was slightly smaller in 1994–2019 than in 1968–1993. The CDHE indicators for the seven geographic subregions of mainland China also showed an upward trend from 1968 to 2019, especially in SWC, NC and EC. The CDHE indicators in CC and EC showed a stronger increasing trend in 1994–2019 than in 1968–1993 (except for $CDHE_{dur}$ in EC). The upward trend of the CHDE indicators in SWC and SC slowed significantly in 1994–2019, and this effect was the most pronounced in SC. Interestingly, we observed that the CDHE indicators in NWC, NC, and NEC showed a decreasing trend in both periods, especially in NEC. Overall, the trend of the CDHE indicators had a lower rate of increase in 1994–2019 than in 1968–1993 or showed a downward trend in mainland China and most geographic subregions (except for CC and EC). These results can be partially attributed to afforestation and reforestation projects carried out in recent years in mainland China. They have resuled in increased vegetation cover, lower summer temperatures, and higher summer precipitation, ultimately slowing down the occurrence of CDHEs in most parts of mainland China (Chen et al., 2019a; Yu et al., 2020). However, since CC and EC have high anthropogenic activity and strong economic dynamics in mainland China, the urban heat island phenomenon has become prominent in summer in recent years (Shen et al., 2016; Zhu et al., 2014), affecting the cooling and rainfall effects due to vegetation greening and producing a net effect of higher temperatures and less rainfall, intensifying CDHEs.

4. Discussion

It has been shown that $CDHE_{fre}$ is expected to increase 10-fold globally under the highest CO_2 emissions scenario, with a disproportionately negative impact on vegetation and socio-economic productivity by the end of the 21st century. >90 % of the global population may be at increased risk of CDHEs in the future (Yin et al., 2023). Continued warming accelerates the variability of climate variables, such as temperature and precipitation, and CDHEs tend to occur more suddenly in a shorter period of time. Previous studies have mostly identified CDHEs at monthly or annual scales and did not monitor short-term CDHEs (Feng et al., 2021, Feng et al., 2020; Otkin et al., 2018). Therefore, this study used daily-scale meteorological data to monitor CDHEs at a finer temporal resolution (daily scale). As described in Section 3.2, daily-scale assessment is preferable to monthly-scale momitoring of short-term CDHEs and provides more detail on the evolution of CDHEs, enabling the timely formulation of mitigation strategies in areas with high agricultural dependence and high meteorological hazard risk.

We considered the PAE in the assessment of CDHEs. Heggen (2001) suggested that the precipitation attenuation coefficient range should be 0.80–0.98. To study the effect of the precipitation attenuation coefficient

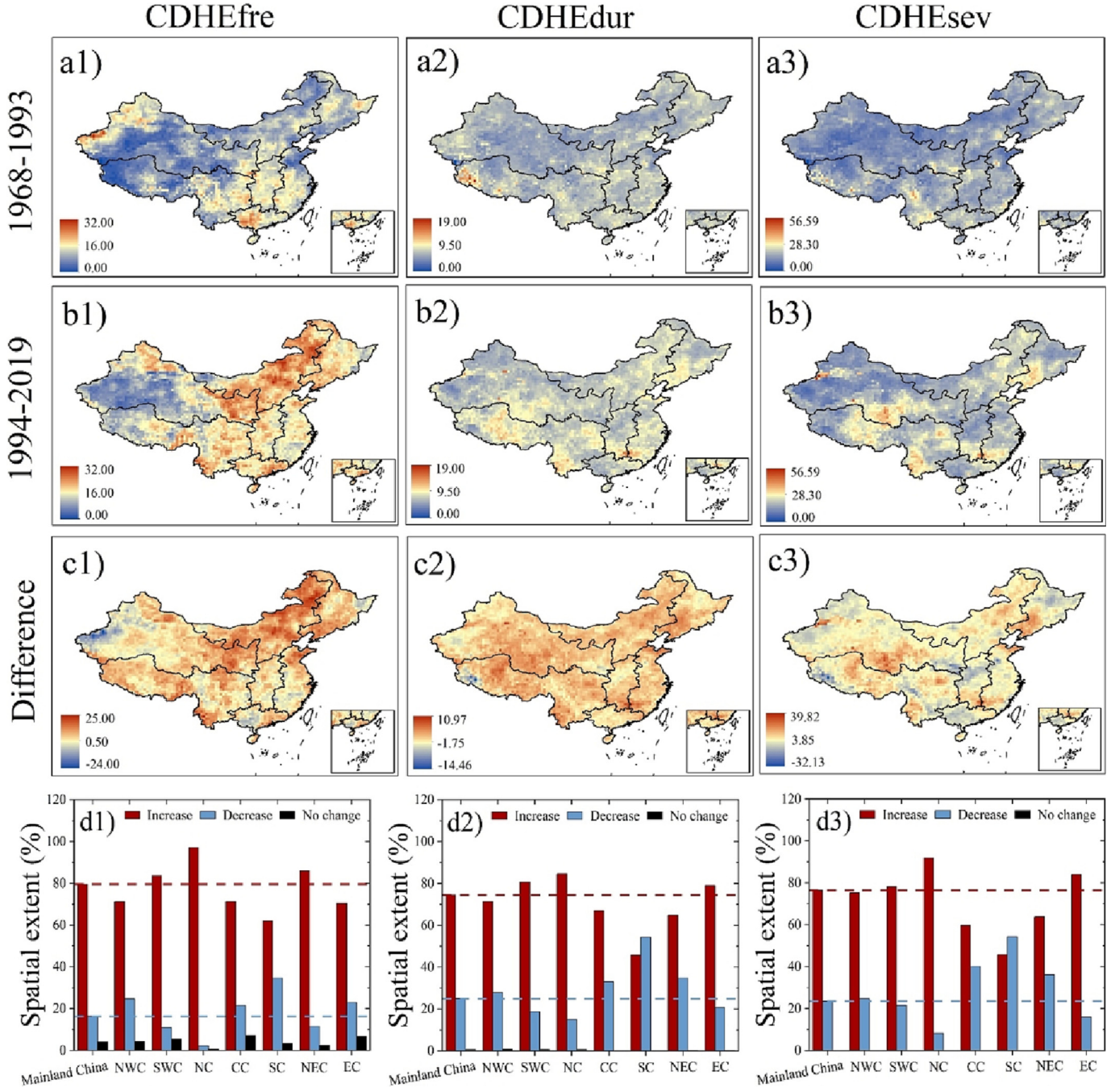

Fig. 8. Differences in the spatial distribution of the CDHE indicators in mainland China between the relatively cold period 1968–1993 and the relatively warm period 1994–2019. The red, blue, and black bars in d1-d3 indicate, respectively, the proportion of areas whose CDHE indicators increased, decreased, and showed no change in the warmer years 1994–2019 compared to the colder years 1968–1993.

on CDHEs, we investigated the spatial distribution of the CDHE indicators in mainland China from 1968 to 2019 with different precipitation attenuation coefficients for a merging threshold of 4 days (Fig. S1). The results showed that the spatial distribution of the CDHE indicators for different combinations of precipitation attenuation coefficients showed a significant positive correlation (Fig. S3). An identical parameter can be used for meteorological drought, which is caused by precipitation, to consider the general characteristics of the soil and land surface (i.e., the general decay effect of the runoff, evapotranspiration, and percolation) (Lu, 2009). We followed the example of Li et al. (2020b) and used a precipitation attenuation coefficient of 0.98 to obtain objective results. However, it is worth noting that different precipitation attenuation coefficients can be used for different locations if the location's soil and surface characteristics (soil texture, vegetation type, land management, land use and land cover change) are considered. However, this strategy requires large amount of data and many experiments; thus, it requires further in-depth research.

Similarly, we assessed the spatial distribution with different merging thresholds when the precipitation attenuation coefficient was 0.98 (the merging thresholds ranged from 4 days to 10 days, Fig. S2). We

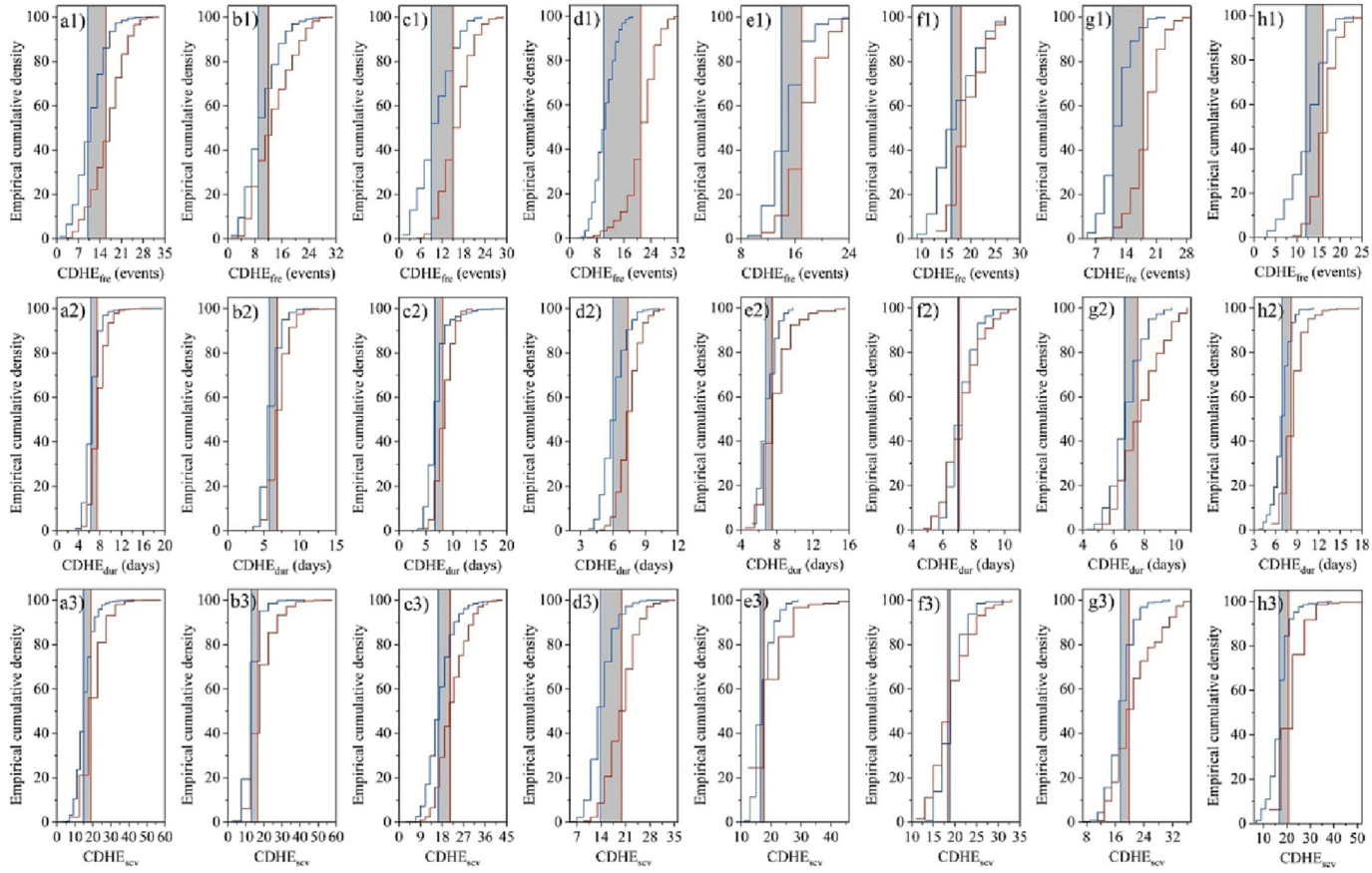

Fig. 9. Statistically significant changes in the empirical cumulative density function (ECDF) and median of the CDHE indicators in mainland China and seven geographic subregions in two periods. The letters a-h in the upper left corner of the graphs indicate mainland China, NWC, SWC, NC, CC, SC, NEC, and EC, respectively. The numbers 1–3 indicate $CDHE_{fre}$, $CDHE_{dur}$, and $CDHE_{sev}$, respectively. The blue horizontal step lines indicate the relatively colder period 1968–1993, and the red horizontal step lines indicate the relatively warmer period 1994–2019. The blue and red vertical lines indicate the median of the CDHE indicators for the two periods, respectively.

found that the difference between the results of the assessment of CDHEs in mainland China was negligible when the merging threshold was 4 to 10 days (Fig. S4). Similar to Mukherjee et al. (2020), we assumed that if two adjacent CDHEs were separated by less than four days, the system would remain under hydrothermal stress. The two CDHEs were merged into a single event based on the criterion that the system could not recover from the state. However, this threshold was based on studies on human mortality due to heatwaves and may be less suitable for studying the effects of CDHEs on ecosystem factors such as vegetation (Curriero et al., 2002; Keellings and Waylen, 2014). If other research objects are investigated, the growth mechanism should be determined first, followed by setting a merging threshold of the CDHEs.

Previous studies analyzed the spatiotemporal variation of CDHEs by dividing the study period into two periods of equal time, ignoring the potential influence of the background temperature (Wang et al., 2021; Zhou and Liu, 2018). We divided the study period into warmer and colder periods and confirmed that the growth rates of CDHEs in mainland China and most geographical regions were lower or showed a decreasing trend in the warm period than in the cold period (Fig. 10), although climate warming greatly promoted the magnitude of CDHE indicators in mainland China (Figs. 8 and 9). This result may be due to the reforestation projects in recent years. Chen et al. (2019a) showed that China has led the global greening of vegetation by implementing many large ecological projects in recent years. A study assessing the impact of these projects on regional climate showed that the significant increase in vegetation greening led to a decrease in summer temperatures and an increase in precipitation in mainland China (Yu et al., 2020). These studies partially explain the recent mitigation of CDHEs in mainland China. However, more future studies are needed to investigate the mechanisms behind the spatio-temporal variability of CDHEs from the perspectives of large-scale circulation patterns and land-atmosphere coupling.

5. Conclusion

We established a novel daily-scale assessment framework for CDHEs that considered the PAE and EM and used it in a systematic investigation of the spatiotemporal variations of the $CDHE_{spa}$, $CDHE_{fre}$, $CDHE_{dur}$, and $CDHE_{sev}$ in mainland China from 1968 to 2019. The results showed that the spatial distribution of the CDHE indicators in mainland China was strongly heterogeneous in 1968–2019, with an increasing number of regions exposed to more frequent, more persistent and more severe CDHEs. Warming substantially contributed to CDHEs in mainland China compared to the cooler 1968–1993 period, but the CDHE indicators grew at a slower rate in the warmer 1994–2019 period. There were significant regional differences in the spatiotemporal variation of CDHEs in mainland China. It is worth noting that daily-scale assessments of CDHEs can provide decision-makers with detailed information on the CDHE evolution for operational monitoring. Ignoring the PAE and EM significantly altered the spatial distribution and magnitude of the CDHE indicators. This study emphasizes the need to consider the

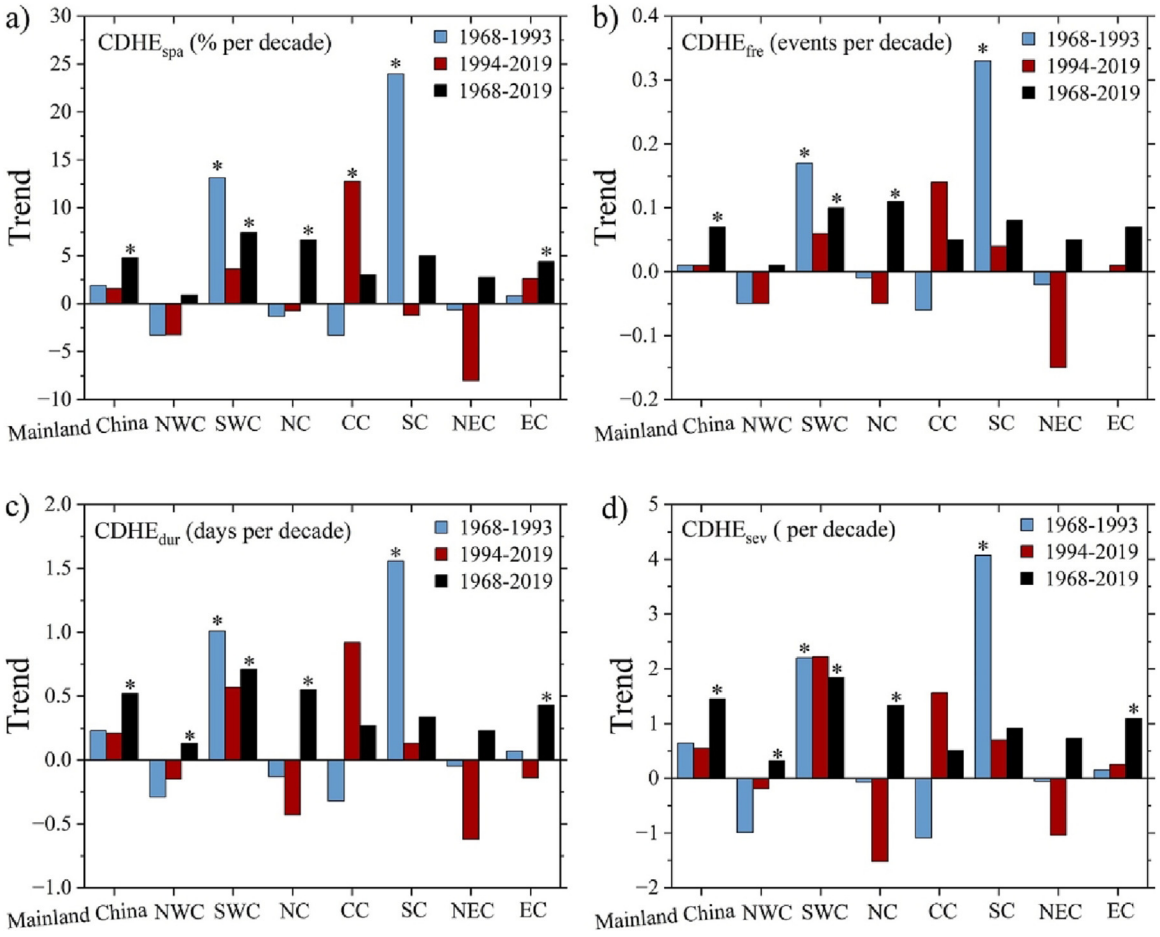

Fig. 10. Interannual trends of CDHE indicators for mainland China and its seven geographical subregions for 1968–1993, 1994–2019, and 1968–2019. The CDHE indicators were calculated at the grid scale for each year, and a multi-year time series of each CDHE indicator was obtained after spatial averaging. The trends were assessed by Sen's slope, and the MK test was used to determine the statistical significance at the 95 % confidence level. The * symbols on the bar graphs represent trends that are significant at the 95 % confidence level.

PAE and EM in CDHE assessments and conduct assessments on a daily scale, contributing significantly to previous CDHE studies. The results of this study can provide valuable theoretical guidance for CDHE risk management, and the proposed CDHEs evaluation framework can be extended to larger spatial scales.

Supplementary data to this article can be found online at https://doi.org/10.1016/j.scitotenv.2023.162366.

CRediT authorship contribution statement

Lin Zhao: Conceptualization, Methodology, Funding acquisition, Writing – original draft, Writing – review & editing. **Xinxin Li:** Conceptualization, Methodology, Formal analysis, Visualization, Writing – original draft, Writing – review & editing. **Zhijiang Zhang:** Conceptualization, Methodology, Investigation, Writing – review & editing. **Moxi Yuan:** Conceptualization, Methodology, Investigation, Writing – review & editing. **Shao Sun:** Investigation, Writing – review & editing. **Sai Qu:** Investigation, Writing – review & editing. **Mengjie Hou:** Investigation, Writing – review & editing. **Dan Lu:** Investigation, Writing – review & editing. **Yajuan Zhou:** Investigation, Writing – review & editing. **Aiwen Lin:** Investigation, Writing – review & editing.

Data availability

Data will be made available on request.

Declaration of competing interest

The authors declare that they have no known competing financial interests or personal relationships that could have appeared to influence the work reported in this paper.

Acknowledgements

This research was funded by National Key Research and Development Program of China (grant number 2019YFE0127600), National Natural Science Foundation of China (grant number U22B2011, 41301586) and Fundamental Research Funds for the Central Universities (grant number 2042022gf0012).

References

AghaKouchak, A., Chiang, F., Huning, L., Love, C., Mallakpour, I., Mazdiyasni, O., Moftakhari, H., Papalexiou, S., Ragno, E., Sadegh, M., 2020. Climate extremes and compound hazards in a warming world. Annu. Rev. Earth Planet. Sci. 48, 519–548. https://doi.org/10.1146/annurev-earth-071719-055228.

Alizadeh, M., Adamowski, J., Nikoo, M., AghaKouchak, A., Dennison, P., Sadegh, M., 2020. A century of observations reveals increasing likelihood of continental-scale compound dry-hot extremes. Sci. Adv. 6. https://doi.org/10.1126/sciadv.aaz4571.

Bevacqua, E., Zappa, G., Lehner, F., Zscheischler, J., 2022. Precipitation trends determine future occurrences of compound hot-dry events. Nat. Clim. Chang. 12, 350–355. https://doi.org/10.1038/s41558-022-01309-5.

Chen, C., Park, T., Wang, X., Piao, S., Xu, B., Chaturvedi, R., Fuchs, R., Brovkin, V., Ciais, P., Fensholt, R., Tommervik, H., Bala, G., Zhu, Z., Nemani, R., Myneni, R., 2019a. China and

India lead in greening of the world through land-use management. Nat. Sustain. 2, 122–129. https://doi.org/10.1038/s41893-019-0220-7.
Chen, L., Chen, X., Cheng, L., Zhou, P., Liu, Z., 2019b. Compound hot droughts over China: identification, risk patterns and variations. Atmos. Res. 227, 210–219. https://doi.org/10.1016/j.atmosres.2019.05.009.
Curriero, F., Heiner, K., Samet, J., Zeger, S., Strug, L., Patz, J., 2002. Temperature and mortality in 11 cities of the eastern United States. Am. J. Epidemiol. 155, 80–87. https://doi.org/10.1093/aje/155.1.80.
Dai, A., 2012. Erratum: drought under global warming: a review. Wiley Interdiscip. Rev.-Clim. Chang. 3, 617. https://doi.org/10.1002/wcc.190.
Feng, S., Wu, X., Hao, Z., Hao, Y., Zhang, X., Hao, F., 2020. A database for characteristics and variations of global compound dry and hot events. Weather Clim. Extremes 30. https://doi.org/10.1016/j.wace.2020.100299.
Feng, S., Hao, Z., Zhang, X., Hao, F., 2021. Changes in climate-crop yield relationships affect risks of crop yield reduction. Agric. For. Meteorol. 304. https://doi.org/10.1016/j.agrformet.2021.108401.
Geirinhas, J., Russo, A., Libonati, R., Sousa, P., Miralles, D., Trigo, R., 2021. Recent increasing frequency of compound summer drought and heatwaves in Southeast Brazil. Environ. Res. Lett. 16. https://doi.org/10.1088/1748-9326/abe0eb.
Grumm, R., 2011. The central european and russian heat event of july-august 2010. Bull. Am. Meteorol. Soc. 92, 1285–1296. https://doi.org/10.1175/2011BAMS3174.1.
Guion, A., Turquety, S., Polcher, J., Pennel, R., Bastin, S., Arsouze, T., 2022. Droughts and heatwaves in the Western Mediterranean: impact on vegetation and wildfires using the coupled WRF-ORCHIDEE regional model (RegIPSL). Clim. Dyn. 58, 2881–2903. https://doi.org/10.1007/s00382-021-05938-y.
Guntu, R., Agarwal, A., 2021. Disentangling increasing compound extremes at regional scale during Indian summer monsoon. Sci. Rep. 11. https://doi.org/10.1038/s41598-021-95775-0.
Hamed, R., van Loon, A., Aerts, J., Coumou, D., 2021. Impacts of compound hot-dry extremes on US soybean yields. Earth Syst. Dyn. 12, 1371–1391. https://doi.org/10.5194/esd-12-1371-2021.
Hansen, J., Sato, M., Ruedy, R., 2012. Perception of climate change. Proc. Natl. Acad. Sci. U. S. A. 109, E2415–E2423. https://doi.org/10.1073/pnas.1205276109.
Hao, Z., Hao, F., Singh, V., Zhang, X., 2019. Statistical prediction of the severity of compound dry-hot events based on El Nino-southern oscillation. J. Hydrol. 572, 243–250. https://doi.org/10.1016/j.jhydrol.2019.03.001.
Hao, Y., Hao, Z., Feng, S., Zhang, X., Hao, F., 2020a. Response of vegetation to El Nino-southern oscillation (ENSO) via compound dry and hot events in southern Africa. Glob. Planet. Chang. 195. https://doi.org/10.1016/j.gloplacha.2020.103358.
Hao, Y., Hao, Z., Fu, Y., Feng, S., Zhang, X., Wu, X., Hao, F., 2021. Probabilistic assessments of the impacts of compound dry and hot events on global vegetation during growing seasons. Environ. Res. Lett. 16. https://doi.org/10.1088/1748-9326/ac1015.
Hao, Z., Hao, F., Xia, Y., Feng, S., Sun, C., Zhang, X., Fu, Y., Hao, Y., Zhang, Y., Meng, Y., 2022. Compound droughts and hot extremes: characteristics, drivers, changes, and impacts. Earth Sci. Rev. 235, 104241. https://doi.org/10.1016/j.earscirev.2022.104241.
Hao, Z., Li, W., Singh, V., Xia, Y., Zhang, X., Hao, F., 2020b. Impact of dependence changes on the likelihood of hot extremes under drought conditions in the United States. J. Hydrol. 581. https://doi.org/10.1016/j.jhydrol.2019.124410.
Hayes, M., Svoboda, M., Wall, N., Widhalm, M., 2011. The Lincoln declaration on drought indiceS. Bull. Am. Meteorol. Soc. 92, 485–488. https://doi.org/10.1175/2010BAMS3103.1.
Heggen, R., 2001. Normalized antecedent precipitation index. J. Hydrol. Eng. 6, 377–381. https://doi.org/10.1061/(ASCE)1084-0699(2001)6:5(377).
Keellings, D., Waylen, P., 2014. Increased risk of heat waves in Florida: characterizing changes in bivariate heat wave risk using extreme value analysis. Appl. Geogr. 46, 90–97. https://doi.org/10.1016/j.apgeog.2013.11.008.
Kendall, M., 1975. Rank Correlation Methods. Charles Griffin. London. 202, p. 15.
Konapala, G., Mishra, A., 2020. Quantifying climate and catchment control on hydrological drought in the continental United States. Water Resour. Res. 56. https://doi.org/10.1029/2018WR024620.
Kumar, S., Zwiers, F., Dirmeyer, P., Lawrence, D., Shrestha, R., Werner, A., 2016. Terrestrial contribution to the heterogeneity in hydrological changes under global warming. Water Resour. Res. 52, 3127–3142. https://doi.org/10.1002/2016WR018607.
Lee Rodgers, J., Nicewander, W., 1988. Thirteen ways to look at the correlation coefficient. Am. Stat. 42, 59–66.
Leonard, M., Westra, S., Phatak, A., Lambert, M., van den Hurk, B., McInnes, K., Risbey, J., Schuster, S., Jakob, D., Stafford-Smith, M., 2014. A compound event framework for understanding extreme impacts. Wiley interdiscip. Rev.-Clim. Chang. 5, 113–128. https://doi.org/10.1002/wcc.252.
Li, X., Li, Y., Chen, A., Gao, M., Slette, I., Piao, S., 2019. The impact of the 2009/2010 drought on vegetation growth and terrestrial carbon balance in Southwest China. Agric. For. Meteorol. 269, 239–248. https://doi.org/10.1016/j.agrformet.2019.01.036.
Li, J., Wang, Z., Wu, X., Chen, J., Guo, S., Zhang, Z., 2020a. A new framework for tracking flash drought events in space and time. Catena 194. https://doi.org/10.1016/j.catena.2020.104763.
Li, J., Wang, Z., Wu, X., Xu, C., Guo, S., Chen, X., 2020b. Toward monitoring short-term droughts using a novel daily scale, standardized antecedent precipitation evapotranspiration index. J. Hydrometeorol. 21, 891–908. https://doi.org/10.1175/JHM-D-19-0298.1.
Li, H., Li, Y., Huang, G., Sun, J., 2021a. Quantifying effects of compound dry-hot extremes on vegetation in Xinjiang (China) using a vine-copula conditional probability model. Agric. For. Meteorol. 311. https://doi.org/10.1016/j.agrformet.2021.108658.
Li, J., Wang, Z., Wu, X., Zscheischler, J., Guo, S., Chen, X., 2021b. A standardized index for assessing sub-monthly compound dry and hot conditions with application in China. Hydrol. Earth Syst. Sci. 25, 1587–1601. https://doi.org/10.5194/hess-25-1587-2021.
Li, X., Wang, Y., Lu, X., Yan, J., 2021c. Diagnosing the impacts of climate extremes on the interannual variations of carbon fluxes of a subtropical evergreen mixed forest. Agric. For. Meteorol. 307. https://doi.org/10.1016/j.agrformet.2021.108507.
Li, E., Zhao, J., Pullens, J., Yang, X., 2022. The compound effects of drought and high temperature stresses will be the main constraints on maize yield in Northeast China. Sci. Total Environ. 812. https://doi.org/10.1016/j.scitotenv.2021.152461.
Liu, Z., Zhou, W., 2021. The 2019 autumn hot drought over the middle-lower reaches of the Yangtze River in China: early propagation, process evolution, and concurrence. J. Geophys. Res.-Atmos. 126. https://doi.org/10.1029/2020JD033742.
Lu, E., 2009. Determining the start, duration, and strength of flood and drought with daily precipitation: rationale. Geophys. Res. Lett. 36. https://doi.org/10.1029/2009GL038817.
Lu, E., Luo, Y., Zhang, R., Wu, Q., Liu, L., 2011. Regional atmospheric anomalies responsible for the 2009–2010 severe drought in China. J. Geophys. Res.-Atmos. 116. https://doi.org/10.1029/2011JD015706.
Lu, E., Cai, W., Jiang, Z., Zhang, Q., Zhang, C., Higgins, R., Halpert, M.S., 2014. The day-to-day monitoring of the 2011 severe drought in China. Clim. Dyn. 43, 1–9. https://doi.org/10.1007/s00382-013-1987-2.
Mann, H., 1945. Nonparametric tests against trend. Econometrica 245–259.
Manning, C., Widmann, M., Bevacqua, E., van Loon, A., Maraun, D., Vrac, M., 2019. Increased probability of compound long-duration dry and hot events in Europe during summer (1950–2013). Environ. Res. Lett. 14. https://doi.org/10.1088/1748-9326/ab23bf.
Mazdiyasni, O., AghaKouchak, A., 2015. Substantial increase in concurrent droughts and heatwaves in the United States. Proc. Natl. Acad. Sci. U. S. A. 112, 11484–11489. https://doi.org/10.1073/pnas.1422945112.
Mishra, A., Singh, V., 2010. A review of drought concepts. J. Hydrol. 391, 204–216. https://doi.org/10.1016/j.jhydrol.2010.07.012.
Mu, M., de Kauwe, M., Ukkola, A., Pitman, A., Guo, W., Hobeichi, S., Briggs, P., 2021. Exploring how groundwater buffers the influence of heatwaves on vegetation function during multi-year droughts. Earth Syst. Dynam. 12, 919–938. https://doi.org/10.5194/esd-12-919-2021.
Mukherjee, S., Mishra, A., 2021. Increase in compound drought and heatwaves in a warming world. Geophys. Res. Lett. 48. https://doi.org/10.1029/2020GL090617.
Mukherjee, S., Ashfaq, M., Mishra, A., 2020. Compound drought and heatwaves at a global scale: the role of natural climate variability-associated synoptic patterns and land-surface energy budget anomalies. J. Geophys. Res.-Atmos. 125. https://doi.org/10.1029/2019JD031943.
Otkin, J., Svoboda, M., Hunt, E., Ford, T., Andersoson, M., Hain, C., Basara, J., 2018. FLASH DROUGHTS a review and assessment of the challenges imposed by rapid-onset droughts in the United States. Bull. Am. Meteorol. Soc. 99, 911–919. https://doi.org/10.1175/BAMS-D-17-0149.1.
Pendergrass, A., Meehl, G., Pulwarty, R., Hobbins, M., Hoell, A., AghaKouchak, A., Bonfils, C., Gallant, A., Hoerling, M., Hoffmann, D., Kaatz, L., Lehner, F., Llewellyn, D., Mote, P., Neale, R., Overpeck, J., Sheffield, A., Stahl, K., Svoboda, M., Wheeler, M., Wood, A., Woodhouse, C., 2020. Flash droughts present a new challenge for subseasonal-to-seasonal prediction. Nat. Clim. Chang. 10, 191–199. https://doi.org/10.1038/s41558-020-0709-0.
Ribeiro, A., Russo, A., Gouveia, C., Pascoa, P., Zscheischler, J., 2020. Risk of crop failure due to compound dry and hot extremes estimated with nested copulas. Biogeosciences 17, 4815–4830. https://doi.org/10.5194/bg-17-4815-2020.
Ridder, N., Pitman, A., Westra, S., Ukkola, A., Hong, X., Bador, M., Hirsch, A., Evans, J., di Luca, A., Zscheischler, J., 2020. Global hotspots for the occurrence of compound events. Nat. Commun. 11. https://doi.org/10.1038/s41467-020-19639-3.
Ridder, N., Ukkola, A., Pitman, A., Perkins-Kirkpatrick, S., 2022. Increased occurrence of high impact compound events under climate change. npj Clim. Atmos. Sci. 5. https://doi.org/10.1038/s41612-021-00224-4.
Robock, A., Vinnikov, K., Srinivasan, G., Entin, J., Hollinger, S., Speranskaya, N., Liu, S., Namkhai, A., 2000. The global soil moisture data Bank. Bull. Amer. Meteorol. Soc. 81, 1281–1299. https://doi.org/10.1175/1520-0477(2000)081<1281:TGSMDB>2.3.CO;2.
Sankarasubramanian, A., Wang, D., Archfield, S., Reitz, M., Vogel, R., Mazrooei, A., Mukhopadhyay, S., 2020. HESS opinions: beyond the long-term water balance: evolving Budyko's supply-demand framework for the anthropocene towards a global synthesis of land-surface fluxes under natural and human-altered watersheds. Hydrol. Earth Syst. Sci. 24, 1975–1984. https://doi.org/10.5194/hess-24-1975-2020.
Sen, P., 1968. Estimates of the regression coefficient based on Kendall's tau. J. Am. Stat. Assoc. 63, 1379–1389.
Shaposhnikov, D., Revich, B., Bellander, T., Bedada, G., Bottai, M., Kharkova, T., Kvasha, E., Lezina, E., Lind, T., Semutnikova, E., Pershagen, G., 2014. Mortality related to air pollution with the Moscow heat wave and wildfire of 2010. Epidemiology 25, 359–364. https://doi.org/10.1097/EDE.0000000000000090.
Sharma, S., Mujumdar, P., 2017. Increasing frequency and spatial extent of concurrent meteorological droughts and heatwaves in India. Sci. Rep. 7. https://doi.org/10.1038/s41598-017-15896-3.
Shen, H., Huang, L., Zhang, L., Wu, P., Zeng, C., 2016. Long-term and fine-scale satellite monitoring of the urban heat island effect by the fusion of multi-temporal and multi-sensor remote sensed data: a 26-year case study of the city of Wuhan in China. Remote Sens. Environ. 172, 109–125. https://doi.org/10.1016/j.rse.2015.11.005.
Shi, Z., Jia, G., Zhou, Y., Xu, X., Jiang, Y., 2021. Amplified intensity and duration of heatwaves by concurrent droughts in China. Atmos. Res. 261. https://doi.org/10.1016/j.atmosres.2021.105743.
Stagge, J., Tallaksen, L., Gudmundsson, L., van Loon, A., Stahl, K., 2015. Candidate distributions for climatological drought indices (SPI and SPEI). Int. J. Climatol. 35, 4027–4040. https://doi.org/10.1002/joc.4267.
Sutanto, S., Vitolo, C., di Napoli, C., D'Andrea, M., van Lanen, H., 2020. Heatwaves, droughts, and fires: exploring compound and cascading dry hazards at the pan-European scale. Environ. Int. 134. https://doi.org/10.1016/j.envint.2019.105276.

Svoboda, M., LeComte, D., Hayes, M., Heim, R., Gleason, K., Angel, J., Rippey, B., Tinker, R., Palecki, M., Stooksbury, D., Miskus, D., Stephens, S., 2002. The drought monitor. Bull. Am. Meteorol. Soc. 83, 1181–1190. https://doi.org/10.1175/1520-0477-83.8.1181.

Turner, S., Voisin, N., Fazio, J., Hua, D., Jourabchi, M., 2019. Compound climate events transform electrical power shortfall risk in the Pacific northwest. Nat. Commun. 10. https://doi.org/10.1038/s41467-018-07894-4.

Wang, R., Lu, G., Ning, L., Yuan, L., Li, L., 2021. Likelihood of compound dry and hot extremes increased with stronger dependence during warm seasons. Atmos. Res. 260. https://doi.org/10.1016/j.atmosres.2021.105692.

Wen, Y., Liu, X., Yang, J., Lin, K., Du, G., 2019. NDVI indicated inter-seasonal non-uniform time-lag responses of terrestrial vegetation growth to daily maximum and minimum temperature. Glob. Planet. Chang. 177, 27–38. https://doi.org/10.1016/j.gloplacha.2019.03.010.

Witte, J., Douglass, A., da Silva, A., Torres, O., Levy, R., Duncan, B., 2011. NASA A-train and Terra observations of the 2010 Russian wildfires. Atmos. Chem. Phys. 11, 9287–9301. https://doi.org/10.5194/acp-11-9287-2011.

Wu, D., Zhao, X., Liang, S., Zhou, T., Huang, K., Tang, B., Zhao, W., 2015. Time-lag effects of global vegetation responses to climate change. Glob. Chang. Biol. 21, 3520–3531. https://doi.org/10.1111/gcb.12945.

Wu, X., Hao, Z., Hao, F., Zhang, X., 2019. Variations of compound precipitation and temperature extremes in China during 1961–2014. Sci. Total Environ. 663, 731–737. https://doi.org/10.1016/j.scitotenv.2019.01.366.

Wu, X., Hao, Z., Zhang, X., Li, C., Hao, F., 2020. Evaluation of severity changes of compound dry and hot events in China based on a multivariate multi-index approach. J. Hydrol. 583. https://doi.org/10.1016/j.jhydrol.2020.124580.

Yin, J., Gentine, P., Slater, L., Gu, L., Pokhrel, Y., Hanasaki, N., Guo, S., Xiong, L., Schlenker, W., 2023. Future socio-ecosystem productivity threatened by compound drought–heatwave events. Nat. Sustain. https://doi.org/10.1038/s41893-022-01024-1.

Yu, L., Liu, Y., Liu, T., Yan, F., 2020. Impact of recent vegetation greening on temperature and precipitation over China. Agric. For. Meteorol. 295. https://doi.org/10.1016/j.agrformet.2020.108197.

Yuan, X., Wang, L., Wu, P., Ji, P., Sheffield, J., Zhang, M., 2019. Anthropogenic shift towards higher risk of flash drought over China. Nat. Commun. 10. https://doi.org/10.1038/s41467-019-12692-7.

Yue, S., Wang, C., 2002. Applicability of prewhitening to eliminate the influence of serial correlation on the Mann-Kendall test. Water Resour. Res. 38. https://doi.org/10.1029/2001WR000861.

Zhou, P., Liu, Z., 2018. Likelihood of concurrent climate extremes and variations over China. Environ. Res. Lett. 13. https://doi.org/10.1088/1748-9326/aade9e.

Zhou, S., Zhang, Y., Williams, A., Gentine, P., 2019. Projected increases in intensity, frequency, and terrestrial carbon costs of compound drought and aridity events. Sci. Adv. 5. https://doi.org/10.1126/sciadv.aau5740.

Zhu, X., Chen, G., Sha, W., Iwasaki, T., Li, W., Wen, Z., 2014. The role of rapid urbanization in surface warming over eastern China. Int. J. Remote Sens. 35, 8295–8308. https://doi.org/10.1080/01431161.2014.985397.

Zscheischler, J., Michalak, A., Schwalm, C., Mahecha, M., Huntzinger, D., Reichstein, M., Berthier, G., Ciais, P., Cook, R., El-Masri, B., Huang, M., Ito, A., Jain, A., King, A., Lei, H., Lu, C., Mao, J., Peng, S., Poulter, B., Ricciuto, D., Shi, X., Tao, B., Tian, H., Viovy, N., Wang, W., Wei, Y., Yang, J., Zeng, N., 2014. Impact of large-scale climate extremes on biospheric carbon fluxes: an intercomparison based on MsTMIP data. Glob. Biogeochem. Cycl. 28, 585–600. https://doi.org/10.1002/2014GB004826.

Zscheischler, J., Westra, S., van den Hurk, B., Seneviratne, S., Ward, P., Pitman, A., AghaKouchak, A., Bresch, D., Leonard, M., Wahl, T., Zhang, X., 2018. Future climate risk from compound events. Nat. Clim. Chang. 8, 469–477. https://doi.org/10.1038/s41558-018-0156-3.

Zscheischler, J., Martius, O., Westra, S., Bevacqua, E., Raymond, C., Horton, R., van den Hurk, B., AghaKouchak, A., Jezequel, A., Mahecha, M., Maraun, D., Ramos, A., Ridder, N., Thiery, W., Vignotto, E., 2020. A typology of compound weather and climate events. Nat. Rev. Earth Environ. 1, 333–347. https://doi.org/10.1038/s43017-020-0060-z.